

Shear wave splitting from local events beneath the Ryukyu arc: Trench-parallel anisotropy in the mantle wedge

Maureen D. Long*, Rob D. van der Hilst

*Department of Earth, Atmospheric, and Planetary Sciences, Massachusetts Institute of Technology,
77 Massachusetts Avenue, Cambridge, MA 02139, United States*

Received 31 October 2005; received in revised form 4 January 2006; accepted 5 January 2006

Abstract

We present shear wave splitting measurements from local slab earthquakes at eight seismic stations of the Japanese *F*-net array located in the Ryukyu arc. We obtained high-quality splitting measurements for 70 event-station pairs and found that the majority of the measured fast directions were parallel to the strike of the trench and perpendicular to the convergence direction. Splitting times for individual measurements ranged from 0.25 to 2 s; most values were between 0.75 and 1.25 s. Both the fast directions and the split times were similar to results for teleseismic *S(K)KS* and *S* wave splitting at the same stations, which suggests that the anisotropy is located in the mantle wedge above the slab. We considered several mantle deformation scenarios that would result in predominantly trench-parallel fast directions, and concluded that for the Ryukyu subduction system the most likely explanation for the observations is corner flow in the mantle wedge combined with B-type olivine fabric. In this model, the flow direction in the wedge is perpendicular to the trench, but the fast axes of olivine crystals tend to align perpendicular to the flow direction, resulting in trench-parallel shear wave splitting.

© 2006 Elsevier B.V. All rights reserved.

Keywords: S-wave splitting; Anisotropy; Upper mantle; Japan; Subduction

1. Introduction

Observations of seismic anisotropy in the Earth's upper mantle, such as measurements of shear wave birefringence or splitting, are an important tool for characterizing the style and geometry of tectonic deformation. The measurement and interpretation of shear wave splitting for phases that traverse the upper mantle has shed light on past and present deformation processes in a variety of tectonic settings: for example, mid-ocean ridges (Wolfe and Solomon, 1998), rift

zones (Kendall et al., 2005), continental collisions (Flesch et al., 2005; Lev et al., 2006), strike-slip faults (Özalaybey and Savage, 1995; Ryberg et al., 2005), regions of mantle upwelling (Walker et al., 2001; Xue and Allen, 2005), and stable cratonic regions (Fouch et al., 2004). Shear wave splitting associated with upper mantle anisotropy has also been found to be nearly ubiquitous in subduction zone settings (Ando et al., 1983; Russo and Silver, 1994; Fouch and Fischer, 1996; Sandvol and Ni, 1997; Fischer et al., 1998; Smith et al., 2001; Anderson et al., 2004; Currie et al., 2004), but the interpretation of shear wave splitting measurements in subduction zones is difficult and non-unique.

There are many processes that can contribute to subduction zone anisotropy, including corner flow in the mantle wedge, flow beneath the slab of subducted litho-

* Corresponding author. Tel.: +1 617 253 3589;
fax: +1 617 258 9697.
E-mail address: mlong@mit.edu (M.D. Long).

sphere, flow around the slab edge, the generation and migration of melt, and anisotropic structure in the slab itself or in the overriding plate (for an overview, see Park and Levin, 2002). Because of the ambiguity of which processes are contributing to the observed anisotropy, and because shear wave splitting is a path-integrated measurement with generally poor depth resolution, the interpretation of shear wave splitting measurements in subduction zone settings is still an area of controversy. In particular, the interpretation of fast splitting directions that are parallel to the trench (that is, perpendicular or at a large angle to the convergence direction) is a matter for some debate.

Both trench-parallel and trench-perpendicular fast directions have been observed in subduction zone settings (for a detailed review, see Wiens and Smith, 2003), but trench-parallel fast directions seem to be more common and have been observed or inferred in New Zealand (Marson-Pidgeon et al., 1999), the Aleutians (Yang et al., 1995; Mehl et al., 2003), Japan (Fouch and Fischer, 1996), and Tonga (Fischer and Wiens, 1996), among other regions. These observations of trench-parallel fast directions contradict the predictions of simple corner-flow models for flow in the mantle wedge, in which viscous coupling between the downgoing slab and the overlying wedge material induces flow that is parallel to the convergence direction (e.g., Fischer et al., 2000). However, new laboratory results have shown that when olivine aggregates are deformed under high-stress, low-temperature, water-rich conditions, the fast axes of individual olivine crystals tend to align 90° from the flow direction (Jung and Karato, 2001). These B-type olivine fabrics, in conjunction with trench-perpendicular flow in the mantle wedge, may explain trench-parallel fast directions in some regions (Karato, 2003; Kneller et al., 2005). It is not clear, however, if the stresses, temperatures, and volatile concentrations needed to produce B-type olivine fabric are relevant to large volumes of the mantle wedge.

In a study of teleseismic shear wave splitting at stations of the broadband *F*-net array in Japan, Long and van der Hilst (2005a) reported consistently trench-parallel fast directions in the Ryukyu arc, with split times between 0.65 and 1.2 s. However, the depth extent and location of the anisotropy could not be determined because the study focused mainly on measurements of SKS, SKKS, and teleseismic *S* phases. Here, we report the results of a follow-up study of splitting from local slab events at Ryukyu arc stations (see Fig. 1 for station locations and tectonic setting). The comparison of shear wave splitting in local and teleseismic arrivals allows us to isolate contributions from anisotropy in the mantle wedge. The depth constraint on anisotropy thus provided

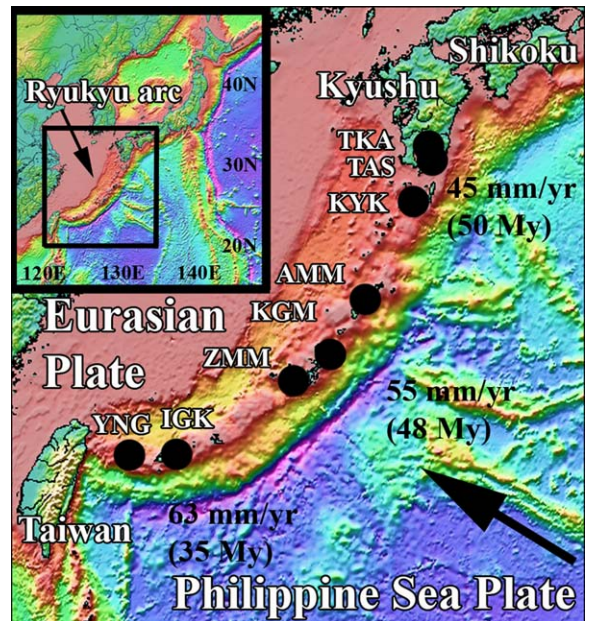


Fig. 1. Tectonic setting of the Ryukyu arc and station locations (black circles). Colors represent topography and seafloor bathymetry from Smith and Sandwell (1997). Large black arrow shows the convergence direction at the trench. Velocities of the Philippine plate relative to Eurasia (from the HS3-Nuvel1A model, Gripp and Gordon, 2002) and seafloor ages quoted in Heuret and Lallemand (2005) are shown at three locations along the arc.

can help discriminate among the various hypotheses for explaining subduction zone anisotropy.

2. Tectonics of the Ryukyu arc

We summarize the geological evolution and tectonic setting of the Ryukyu arc after overviews by Taira (2001) and Schellart et al. (2002). The Ryukyu arc (Fig. 1) is associated with the subduction, initiated at ~ 55 Ma, of the Philippine plate beneath Eurasia at a relative rate of ~ 55 mm/yr. The convergence direction is to the northwest and the trench strikes generally NE-SW, so that along most of the arc there is little or no obliquity in subduction direction (e.g., McCaffrey, 1996). Rifting in the backarc, bounded by the Okinawa Trough to the northwest, started in the late Miocene (Schellart et al., 2002; Letouzey and Kimura, 1985). Slab rollback rates are generally small along most of the arc, with a rate of (southeastward) trench migration of less than 10 mm/yr (Heuret and Lallemand, 2005; Yu and Kuo, 1996; Mazzotti, 1999). However, toward the southernmost part of the arc, where the strike of the trench changes from NE-SW to nearly E-W, there is an increase in subduction obliquity and in the rate of slab rollback. The part of the Ryukyu arc near Taiwan has been stud-

ied extensively (e.g., Kao et al., 2000) but the tectonic setting here is more complicated than in the center of the arc and there is no consensus on how deformation is accommodated.

The morphology of the subducting Philippine slab has been studied using earthquake hypocenter locations (Engdahl et al., 1998; Gudmundsson and Sambridge, 1998) and seismic tomography of the western Pacific (e.g., Widiyantoro et al., 1999; Gorbato and Kennett, 2003; Lebedev and Nolet, 2003; Li et al., 2006), although the slab is generally not well resolved at shallow depths (below ~ 300 km) by the data used in the tomographic inversions. The slab dips at approximately 45° to the northwest, and the dip remains nearly constant along the strike of the trench. The maximum depth of the seismogenic zone decreases from ~ 300 km in the south to ~ 250 km in the north (Gudmundsson and Sambridge, 1998). For studies of the crustal structure of the Ryukyu arc and the adjacent oceanic regions we refer to Iwasaki et al. (1990) and Wang et al. (2004). Analyses of earthquake focal mechanisms and fault geometries (e.g., McCaffrey, 1996; Fournier et al., 2001; Kubo and Fukuyama, 2003) suggest the existence of localized regions of arc-parallel extension along the arc, but it is unclear to what degree, if any, extension in the crust is coupled to deformation in the mantle.

3. Data and methods

We have analyzed data from the eight southernmost stations of *F*-net (Fig. 1), a network of 82 broadband seismic stations in Japan (<http://www.fnet.bosai.go.jp>). With the exception of station YNG, which was not installed until mid-2002, we previously investigated teleseismic shear wave splitting at each of these stations (Long and van der Hilst, 2005a). Among the *F*-net stations throughout Japan, Ryukyu arc stations exhibited some of the largest split times, generally around 1 s or more. Long and van der Hilst (2005a) observed backazimuthal variations in observed splitting patterns, presumably indicating complex anisotropy, at the majority of *F*-net stations, but the Ryukyu stations exhibited splitting patterns consistent with a simple anisotropic model (that is, a single anisotropic layer with a horizontal axis of symmetry).

To understand the origin of the anisotropic signal better we investigate if splitting from events located in the slab itself can help distinguish between anisotropy in the mantle wedge and anisotropy within or beneath the slab of subducted lithosphere. We selected intermediate (70–300 km) depth earthquakes occurring between July 1999 and May 2005. We searched for events at a small distance ($1\text{--}2^\circ$) from each station location to facilitate

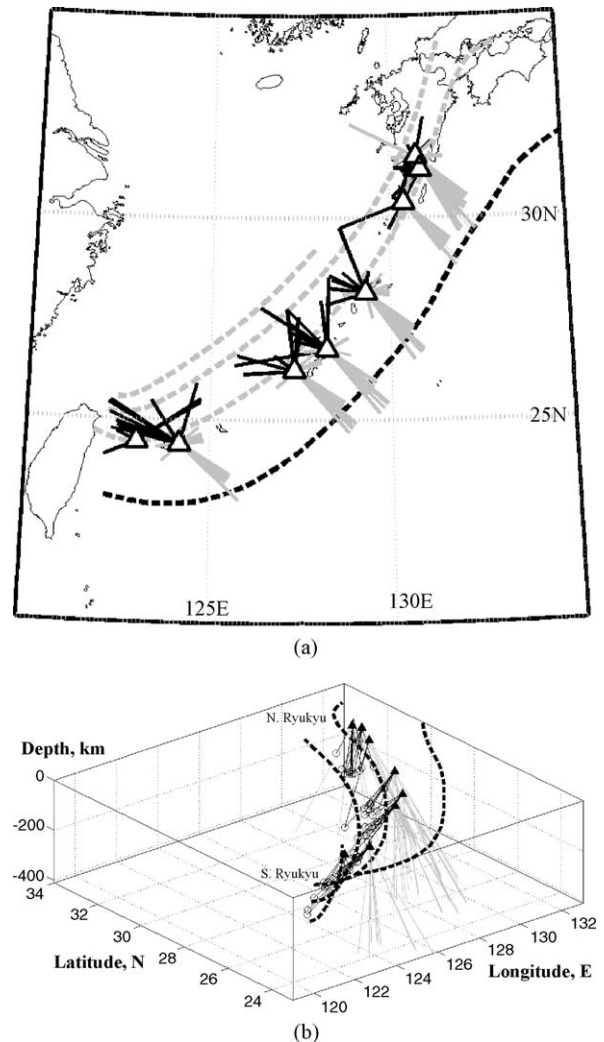


Fig. 2. (a) Map view of raypaths for local events analyzed in this study (black) and teleseismic events (gray) analyzed in Long and van der Hilst (2005a). (b) Three-dimensional sketch of local (black) and teleseismic (gray) raypaths in the upper mantle, looking north along the Ryukyu arc. Raypaths are approximated as straight lines. Local events are marked with open circles.

the interpretation of the results and to ensure that all shear phases arrive within the angular window defined by the critical *P*–*S* conversion angle at the free surface. Fig. 2 depicts the locations of the events and stations used in this study, as well as the approximate raypaths for both the local *S* phases and the teleseismic raypaths from Long and van der Hilst (2005a).

After identifying candidate events for analysis, *S* wave arrivals with high signal-to-noise ratios were selected by visual inspection of the waveforms. Before this inspection we applied two different bandpass filters: one with corner frequencies of 0.02 and 0.125 Hz, which

is the same as used in Long and van der Hilst (2005a), and one with corner frequencies of 0.1 and 1 Hz, similar to the filter used in Levin et al. (2004). Most events had significant energy in one band or the other, but not both. Most *S* arrivals from the local events had more energy in the higher frequencies, but we report splitting results for both the high- and the low-frequency bandpass (0.02–0.125 Hz) because the latter can be more easily compared to the teleseismic splitting reported in Long and van der Hilst (2005a).

Once clear *S* wave arrivals were identified in the data, we applied the cross-correlation method to estimate splitting parameters (Ando et al., 1983; Fukao, 1984). This method grid-searches for the fast direction φ and split time δt that corrects the horizontal seismogram components to the two most nearly identical pulse shapes. We use an implementation of the cross-correlation algorithm described by Levin et al. (1999). Long and van der Hilst (2005b) evaluated the performance of several shear wave splitting methods at Japanese stations and found that this method was generally stable and robust even for complex tectonic regions. We visually checked the corrected particle motion diagrams to ensure near-linearity, and the contour plots of the cross-correlation coefficient for each potential pair of splitting parameters were inspected to ensure the best-fitting (φ , δt) values were well-constrained. We calculated formal errors based on the formulation of Levin et al. (1999). An example of a splitting analysis for a recording at station IGK is shown in Fig. 3.

4. Results

In the high frequency band we obtained a total of 34 well-constrained splitting measurements at the eight stations considered in this study, along with eight well-constrained null measurements (clear *S* arrivals with no discernable splitting). In the low frequency band we obtained 19 measurements and 9 nulls. We list all measurements in table form as Table 1. Individual measurements of fast direction φ and split time δt in each frequency band are plotted in Fig. 4, along with average teleseismic splitting from Long and van der Hilst (2005a).

A striking feature of the low-frequency data set (Fig. 4a) is the preponderance of fast directions that are parallel or sub-parallel to the strike of the trench, which is in agreement with splitting in the teleseismic data. About two-thirds of the fast directions measured in the low frequency band were found to be within 20° of the strike of the trench. Notable exceptions to this trend include measurements made at the two southern-

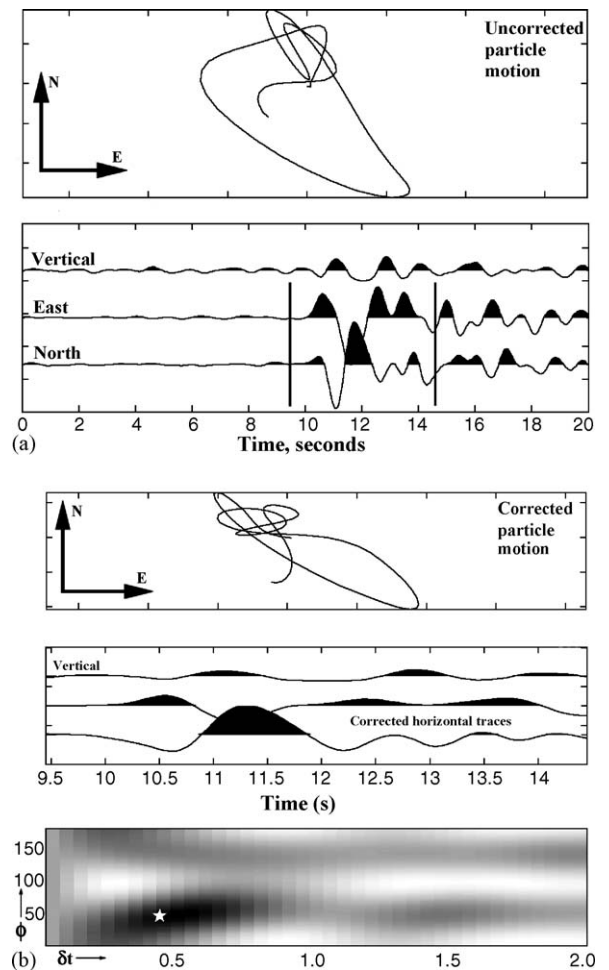


Fig. 3. (a) Uncorrected particle motion (top) and seismogram components (bottom) for a typical high-frequency *S* arrival at station IGK. Vertical bars on the horizontal traces indicate the window used in the splitting analysis. (b) Corrected particle motion (top) and seismogram components (middle) for the best-fitting φ and δt values (46° and 0.45 s, respectively). In the bottom panel, a contour plot of the cross-correlation values is shown. The pair of splitting parameters that maximizes the cross-correlation is marked with a white star.

most stations in the array, YNG and IGK, where there is a great deal of scatter in the measurements, and a few measurements at station ZMM. In the high-frequency band the directions are more variable: compared to measurements at low frequency, we observe more fast directions that are nearly perpendicular or oblique to the strike of the trench (Fig. 4b), and only a slim majority of the measured high-frequency fast directions (53%) is within 20° of trench-parallel. We suggest two possible reasons for the increased scatter. First, a Fresnel zone argument (Alsina and Snieder, 1995) would imply that the low-frequency measurements are sensitive to a larger anisotropic volume than the high-frequency mea-

Table 1

Results of all splitting measurements reported in this study, for high-frequency and low-frequency bandpass filters

Event	Station	Depth (km)	φ ($^{\circ}$)	$d\varphi$ (2σ)	δt (s)	$d\delta t$ (2σ)	Class
High-frequency							
1999.196	AMM	136	N - 68				N
2000.212	AMM	130	6	18	0.45	0.14	O
2001.303	AMM	136	N - 70				N
2002.061	AMM	141	48	20	1.65	0.20	
2002.142	AMM	135	N - 33				N
2003.163	AMM	115	11	15	0.35	0.06	O
2004.295	AMM	95	N - 158				N
2000.148	IGK	245	30	14	1.15	0.12	
2000.206	IGK	124	46	14	0.45	0.13	
2000.315	IGK	109	77	14	1.35	0.10	O
2001.153	IGK	134	9	14	0.80	0.08	O
2002.239	IGK	219	35	12	1.10	0.05	
2002.259	IGK	183	9	20	0.50	0.18	O
2002.277	IGK	134	170	11	1.35	0.06	O
2002.322	IGK	181	11	18	0.50	0.10	O
2003.214	IGK	105	64	9	0.60	0.06	
2005.059	IGK	80	39	15	0.30	0.06	
2005.143	IGK	97	54	20	1.35	0.07	
2000.100	KGM	133	55	22	1.05	0.20	
2000.274	KGM	164	48	20	1.05	0.08	
2002.289	KGM	254	59	14	1.65	0.18	
2003.071	KGM	147	67	15	0.9	0.08	
2001.250	KYK	272	56	14	0.50	0.05	
2002.173	TAS	154	49	13	0.35	0.06	
2002.190	TAS	163	176	11	0.45	0.08	O
2002.298	TAS	121	N - 15				N
2003.204	TAS	163	2	16	0.55	0.10	O
2004.061	TAS	181	15	14	0.75	0.08	O
2000.016	TKA	169	108	17	1.15	0.25	O
2000.093	TKA	159	170	6	0.60	0.03	O
2002.173	TKA	154	103	21	1.05	0.30	O
2002.279	TKA	170	N - 25				N
2002.338	YNG	98	93	22	1.00	0.35	
2003.214	YNG	106	87	14	0.25	0.04	
2003.234	YNG	96	61	24	0.25	0.06	
2002.205	ZMM	110	N - 100				N
2003.061	ZMM	145	100	15	0.95	0.12	O
2003.071	ZMM	148	18	14	0.45	0.08	
2004.242	ZMM	134	102	10	0.75	0.06	O
2004.258	ZMM	122	140	19	1.05	0.08	⊥
2004.262a	ZMM	98	N - 29				N
2004.305	ZMM	89	63	18	0.35	0.09	
Low-frequency							
1999.196	AMM	137	22	21	1.10	0.32	
2001.205	AMM	272	33	18	1.60	0.40	
2001.303	AMM	136	18	18	1.10	0.33	
2000.206	IGK	125	N - 159				N
2001.328	IGK	260	95	17	1.90	0.38	O
2002.259	IGK	183	42	14	1.45	0.16	
2005.143	IGK	98	N - 26				N
2000.117	KGM	163	45	17	1.30	0.28	
2000.180	KGM	108	N - 51				N
2002.283	KGM	162	68	24	1.55	0.60	
2003.048	KGM	189	46	18	1.50	0.40	
2003.071	KGM	148	54	12	1.95	0.5	
2002.298	KYK	121	N - 142				N
2002.298	TAS	121	N - 15				N

Table 1 (Continued)

Event	Station	Depth (km)	φ (°)	$d\varphi$ (2σ)	δt (s)	$d\delta t$ (2σ)	Class
2003.190	TAS	68	68	15	1.45	0.50	
2004.061	TAS	182	20	17	1.10	0.24	
2000.093	TKA	159	53	14	1.15	0.38	
2001.008	TKA	116	N - 47				N
2003.250	YNG	124	21	25	0.60	0.40	⊥
2004.010	YNG	101	121	22	1.4	0.52	O
2005.143	YNG	98	N - 169				N
2003.048	ZMM	189	81	15	1.35	0.32	O
2003.061	ZMM	145	104	18	1.30	0.33	O
2003.071	ZMM	148	81	22	1.65	0.38	O
2004.242	ZMM	133	121	16	1.95	0.42	⊥
2004.262a	ZMM	98	N - 29				N
2004.262b	ZMM	102	39	13	0.85	0.38	
2005.054	ZMM	162	N - 27				N

2σ formal errors on the fast direction φ and split time δt are reported; errors were calculated using the formulation of Levin et al. (1999). Each measurement is classified as null (N), trench-parallel (||), trench-perpendicular (⊥), or oblique (O). For null measurements, we also list the initial polarization direction of the shear wave, in lieu of the fast direction.

surements. Therefore, the low-frequency measurements may tend to “smooth out” small-scale anisotropic heterogeneity that may exist in the mantle wedge whereas the short period data would be more sensitive to it. Second, it has been proposed that for vertically stratified anisotropic structures (for example, crustal anisotropy overlying an anisotropic upper mantle) higher-frequency measurements may be biased toward near-surface structure (Clitheroe and van der Hilst, 1998; Saltzer et al., 2000). Long and van der Hilst (2005a) examined the possibility of crustal contamination in the *F*-net teleseismic shear wave splitting dataset and concluded that an anisotropic signal from the crust, while small, is probably present. It is thus possible that crustal anisotropy contributes to the scatter in our high-frequency splitting measurements.

There is also a noticeable increase in scatter in the southernmost part of the array (stations YNG and IKG) compared to stations located further north. This may be due to a change in crustal anisotropy. However, scatter in the low-frequency data (where we expect the crustal contribution to be much smaller) increases also. Instead, we attribute the increased scatter in the south to more complex anisotropy, which may reflect a southward increase in tectonic complexity. At the southernmost part of the arc the subduction direction in this region becomes oblique to the trench, which causes trench-parallel stretching (Lallemant et al., 1999). Additionally, there may be deformation associated with flow around the slab edge with the transition from subduction at the southern Ryukyu trench to collision in Taiwan (Kao et al., 2000). We focus on the more consistently trench-parallel fast directions observed to the north.

Measured split times range from 0.25 s, which is near the lower detection limit, up to approximately 2 s, with most δt values between 0.75 and 1.25 s. This range of δt values is similar to the range of splitting times observed at Ryukyu stations for teleseismic phases (Long and van der Hilst, 2005a). Along with the similarity of the polarization directions this suggests that the two data sets sample the same source of anisotropy. Fig. 5 shows observed split time with respect to event depth: there is no systematic dependence of split time on earthquake depth, either for the entire dataset (Fig. 5a) or for the trench-parallel measurements only (Fig. 5b). This suggests that most ray paths accumulate a similar split time, regardless of the event focal depth, and, therefore, that the anisotropy is concentrated in the shallower portions of the mantle wedge. If this interpretation is correct a highly anisotropic medium is likely needed to generate the fairly large split times observed. Even if we allow for a contribution from the crust and (thin) lithosphere we would attribute 1 s or more of splitting to a mantle layer of perhaps 60–100 km, which suggests anisotropy up to about 10%.

In general, we find that measurements at low frequencies tend to yield higher split times than measurements at high frequencies (Fig. 5). Similar observations have been made by, for example, Long and van der Hilst (2005b) and Marson-Pidgeon and Savage (1997), but other studies have found different frequency effects, including significant splitting at high frequencies and little splitting at low frequencies (Clitheroe and van der Hilst, 1998; Özalaybey and Chen, 1999) and frequency dependent fast directions with no frequency dependence in split times (Fouch and Fischer, 1998). In our study,

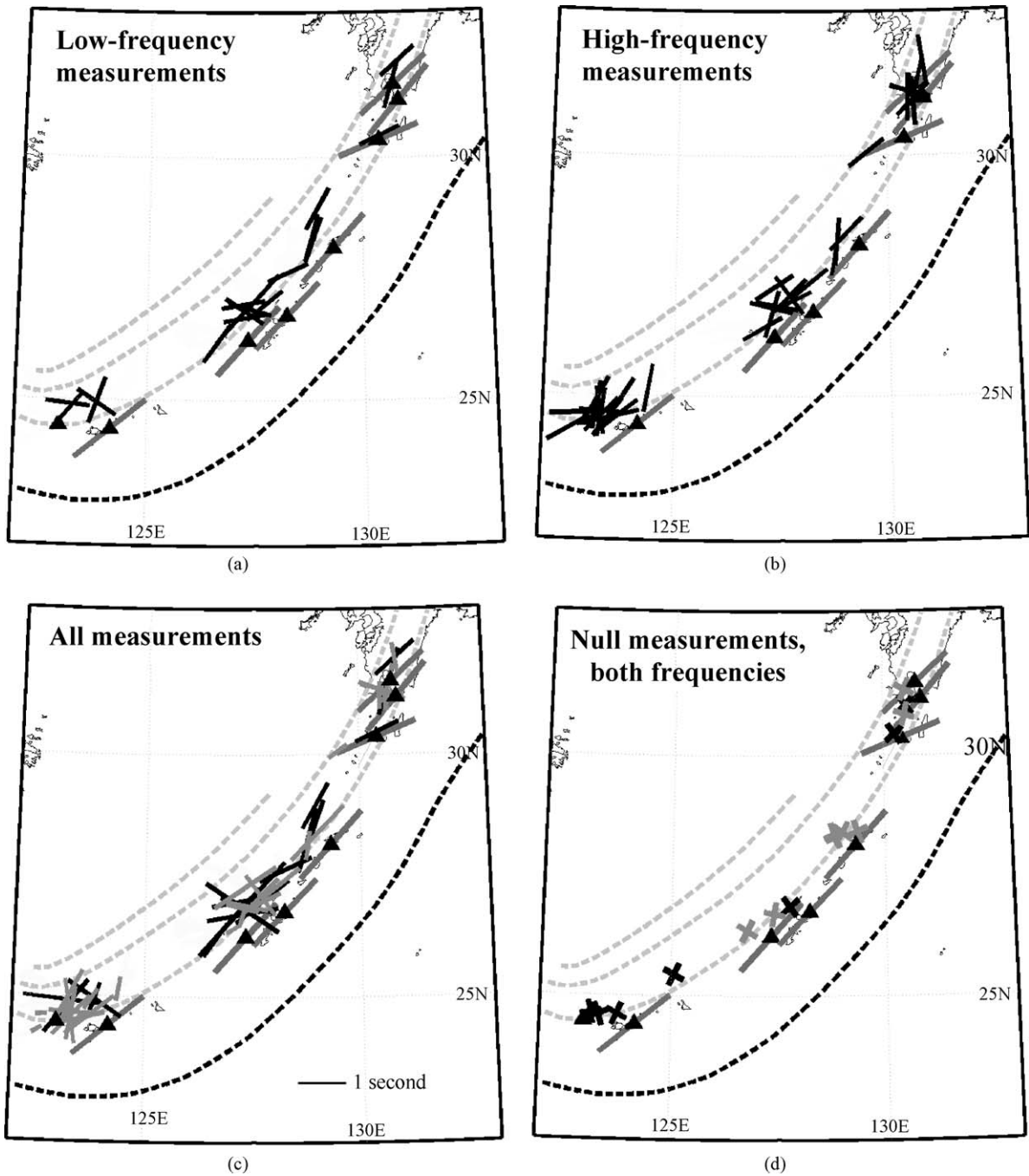


Fig. 4. (a) Fast directions measured in the low frequency band (0.02–0.125 Hz). Individual measurements are plotted as black bars at the midpoint of the raypath. Gray bars plotted at the station locations represent the average teleseismic fast directions from Long and van der Hilst (2005a). Bars have *not* been scaled to the split time in order to emphasize the better-constrained fast directions; bars scaled to the split time are shown in Fig. 4c. (b) Similar to Fig. 4a, for fast directions measured in the high frequency band (0.1–1 Hz). (c) High-frequency measurements are plotted in gray; low-frequency measurements are plotted in black. The length of each bar has been scaled by the split time δt . (d) Null measurements made in the low- (black crosses) and high- (dark gray crosses) frequency bands, plotted at the midpoint of the raypath. Nulls are distributed geographically throughout the arc. The orientation of the crosses correspond to the direction of incoming polarization of the shear wave and the direction 90° from the incoming polarization azimuth.

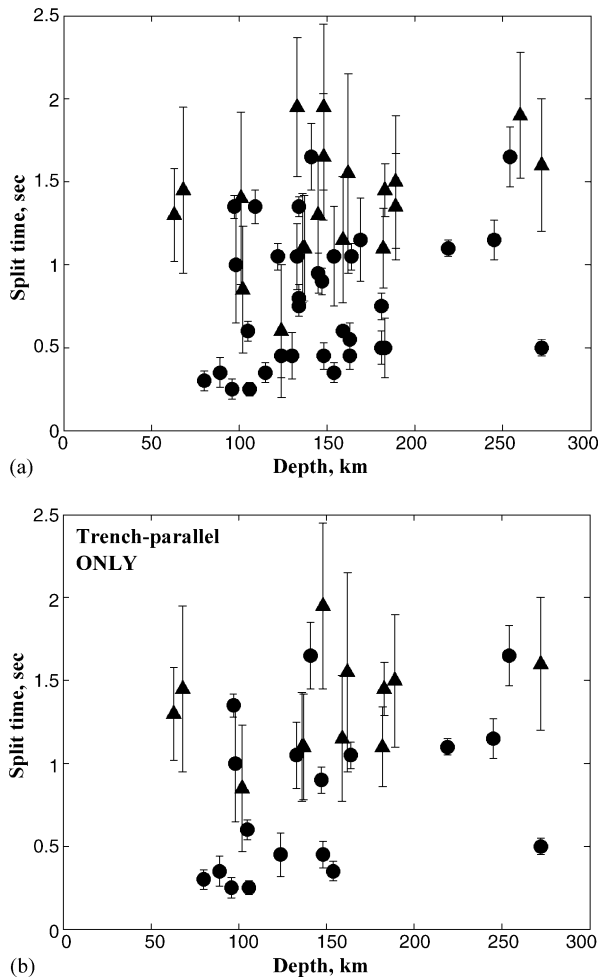


Fig. 5. (a) Plot of measured split time vs. event depth for high-frequency (circles) and low-frequency (triangles) measurements. Error bars are 2σ . (b) Plot of measured split time vs. event depth, for trench-parallel fast directions only.

high-frequency measurements reflect anisotropy in the mantle wedge but a bias towards near-surface anisotropy (Saltzer et al., 2000) may produce smaller delay times (and increased scatter) than measurements made at lower frequencies.

The low- and high-frequency data sets both suggest that there is significant heterogeneity of anisotropic structure, but two first-order conclusions can be drawn from them. First, there is firm evidence for significant anisotropy in the mantle wedge above the subducting Philippine slab beneath the Ryukyu arc. Both the fast directions and split times from local shear waves are remarkably consistent with the teleseismic splitting reported by Long and van der Hilst (2005a). Specifically, even though the teleseismic and local raypaths sample different parts of the mantle wedge (see Fig. 2),

with the teleseismic raypaths sampling the forearc corner of the wedge (as well as the slab itself and the subslab mantle) and the local raypaths sampling the backarc, the character of the anisotropy sampled by these two data sets seems to be similar. While we cannot rule out a contribution to splitting of teleseismic phases from within or beneath the subducting slab, the similarity between the teleseismic and local splitting patterns argues that the teleseismic phases are probably sampling significant anisotropy in the wedge itself. Second, although there is significant scatter, the majority of the fast directions measured in this study are parallel to the trench. This argues for significant trench-parallel anisotropy in the wedge beneath much of the Ryukyu arc, with the possible exception of the two southernmost stations.

5. Models for trench-parallel fast directions

Several hypotheses have been proposed to explain trench-parallel fast directions in subduction zone settings. Russo and Silver (1994) invoked trench-parallel flow beneath the subducting slab associated with slab rollback to explain trench-parallel fast directions in South America. Smith et al. (2001) suggested that trench-parallel fast directions in the Lau Basin result from trench-parallel flow around the slab edge of infiltrating material from the Samoan plume. In subduction zones where the convergence direction is oblique to the strike of the trench, or where there is significant strike-slip motion in the backarc, there may be significant trench-parallel shear in the mantle wedge and a simple corner flow model may not be appropriate (e.g., Hall et al., 2000); this may explain trench-parallel fast directions in such systems. In regions where the morphology of the downgoing slab is complicated, three-dimensional flow patterns in the asthenospheric mantle probably become important, and complex three-dimensional flow may explain trench-parallel fast directions in some subduction systems.

The relative simplicity of the tectonic setting at the Ryukyu arc compared to most subduction zones limits the range of plausible explanations for trench-parallel fast directions in this region. The convergence direction at the Ryukyu arc is perpendicular to the trench (see Fig. 1) except at the southernmost part of the arc, where the strike of the trench rotates from NE-SW to E-W. This implies that transpression in the mantle wedge due to oblique subduction can be ignored as a possible mechanism for trench-parallel fast directions at most Ryukyu stations. The geometry of the Philippine slab beneath Ryukyu as inferred from seismicity (Engdahl et al., 1998; Gudmundsson and Sambridge, 1998) is fairly simple and

is well-described by a two-dimensional model with a slab dip of about 45° (again, with the exception of the southernmost part of the slab). This simple slab morphology tends to argue for a simple flow regime, at least in the interior part of the arc. Finally, although the location of the Ryukyu trench is not completely stationary, along most of the trench the rate of trench migration due to slab rollback is slow compared to a global compilation of trench motions (Heuret and Lallemand, 2005; Yu and Kuo, 1996; Mazzotti, 1999) and the effects of slab rollback on mantle flow patterns are presumably much smaller than for most subduction zones.

In order to explain the predominantly trench-parallel fast directions at the Ryukyu arc stations, we consider several different scenarios for mantle flow and anisotropy generation that are consistent with generally trench-parallel directions. We note that at the southernmost part of the arc a mechanism other than those discussed here may be responsible for the observed anisotropy, such as flow around the slab edge. We emphasize also that although the majority of observed fast directions are trench-parallel, we also found a significant minority of trench-perpendicular or intermediate measurements. Ideally, any successful model for Ryukyu arc anisotropy should be able to explain this subset of measurements as well. In this section we consider four possible scenarios for Ryukyu anisotropy: trench-parallel flow in the mantle wedge, corner flow in the mantle wedge with B-type olivine fabric, shape-preferred orientation of melt pockets, and frozen lithospheric and/or crustal anisotropy that is unrelated to present-day deformation processes.

5.1. Trench-parallel flow in the mantle wedge

Trench-parallel flow beneath the subducting plate has been invoked to explain trench-parallel fast directions in South America (Russo and Silver, 1994; Anderson et al., 2004) and Kamchatka (Peyton et al., 2001); however, we reject such a mechanism here because our local splitting measurements suggest that the trench-parallel anisotropy in the Ryukyu arc has its origin in the mantle wedge, that is, above the plate. Instead, we consider the possibility of trench-parallel flow in the wedge itself. In order to invoke such a model, we must identify a mechanism that would result in consistently trench-parallel flow over a fairly long distance (approximately 800 km along the arc), with trench-parallel strains dominating the mantle wedge flow field. Because we observe trench-parallel fast directions at stations located approximately 100 km from the trench in the interior of the arc (most noticeably station KGM; see Table 1), a mechanism such as flow around the edges

of the slab is probably insufficient. Conder et al. (2002) proposed a model for flow associated with decompression melting in the mantle wedge and suggested that in some arc systems, corner flow may act in concert with trench-parallel flow. It has been suggested (James Conder, Washington University, personal communication) that elevated temperatures in the interior of the mantle wedge lead to a dramatic reduction in viscosity that may form hot, low-viscosity channels whose flow regime is decoupled from the rest of the wedge and the downgoing slab. If such low-viscosity channels form, and if a pressure gradient is applied across the length of the arc, this may drive trench-parallel flow along the arc in a localized channel. A source for such a pressure gradient is somewhat difficult to envision for Ryukyu, however, as the rate of slab rollback is small and appears to be fairly constant over most of the length of the arc (Heuret and Lallemand, 2005). A series of laboratory experiments by Buttle and Olson (1998) investigated the formation of anisotropy due to flow in subduction zones, and they suggested that for systems with simultaneous slab rollback and down-dip motion, fast directions in the wedge should be dominated by the down-dip motion of the slab, and that large amounts of rollback are needed to produce trench-parallel anisotropy anywhere in the system. Therefore, it is difficult to find a mechanism that would produce significant, dominant trench-parallel flow in the Ryukyu mantle wedge, and we conclude that this is an unlikely model to explain the observed trench-parallel splitting. However, this scenario cannot be completely ruled out, and further three-dimensional modeling may clarify the relative importance of trench-parallel and perpendicular flow in subduction systems with slow rollback rates such as Ryukyu.

5.2. Corner flow with B-type olivine fabric

An alternate model for the Ryukyu arc system combines trench-perpendicular corner flow in the mantle wedge (resulting in trench-perpendicular flow directions) with B-type olivine fabric to produce trench-parallel fast splitting directions. This hypothesis for subduction zone anisotropy originated with Jung and Karato (2001), who conducted laboratory experiments on olivine aggregates with significant water content (200–1200 ppm) deformed at high differential stresses (>300 MPa) and found that slip along the [0 0 1] direction was enhanced at these conditions, such that the fast axes of individual olivine crystals tended to be aligned 90° from the shear direction. Examples of B-type fabric in mantle-derived rocks have since been documented by Mizukami et al. (2004) in samples from

the Higashi-akaishi peridotite body in southwest Japan, just northeast of the Ryukyu arc. Subsequent modeling work by Kneller et al. (2005) indicates that B-type fabric conditions may occur in part of the mantle wedge. They find that the forearc mantle may have conditions that favor a B-type fabric (and therefore trench-parallel splitting), and they predict a rapid transition to trench-perpendicular fast directions (associated with A-, C-, or E-type olivine fabric) toward the backarc. The B-type fabric hypothesis has been invoked to explain a transition from trench-parallel splitting in the forearc to trench-perpendicular splitting in the backarc elsewhere in Japan; Nakajima and Hasegawa (2004) observed this apparent rotation at stations located in northern Honshu.

Can the B-type fabric model explain the trench-parallel splitting we observe in Ryukyu? Unfortunately, the *F*-net station distribution is limited to stations located on the volcanic islands themselves, so we do not have good sampling across the entire forearc and backarc region. It is clear from the teleseismic splitting results of Long and van der Hilst (2005a) that there is significant trench-parallel anisotropy in the forearc mantle, which is consistent with the Kneller et al. model. However, the local raypaths examined in this study clearly sample a significant volume of backarc mantle (Fig. 2). Kneller et al. (2005) envision a transition from trench-parallel to trench-perpendicular fast directions located at the volcanic front for a generic subduction zone model. However, we also observe trench-parallel fast directions for rays that sample a larger part of the backarc (see Fig. 4). Our observations could perhaps be reconciled with the models of Kneller et al. if a slight change in their model parameters (such as water content, temperature structure of the incoming and overriding plates, rheological parameters, and the degree of coupling between the slab and the overlying wedge) could move the trench-parallel/trench-perpendicular transition further into the backarc, or if the B-type fabric can exist for a larger range of physical and compositional parameters than inferred experimentally by Jung and Karato (2001). Only a slight shift in this transition point would be required to explain our observations with the B-type model, especially if the anisotropy we observe is generally located on the near-surface portion of the raypaths. It is not immediately obvious what change(s) in model parameters would be required to move the transition point farther into the backarc; we are currently undertaking a detailed comparison of splitting observations in Japan with the models of Kneller et al. (2005), and further modeling of B-type fabric may also be required to elucidate this point. It also remains to be demonstrated through modeling and experiments that a region of B-type fabric in the mantle

wedge can produce split times on the order of the ~ 1.5 s or more that we observe. We note, finally, that some of the measured trench-perpendicular and intermediate fast directions are not inconsistent with the B-type fabric hypothesis if raypaths sample trench-perpendicular fast directions further into the backarc, or if they sample the transition from B- to A-, C-, or E-type fabric regimes.

5.3. Shape-preferred orientation (SPO) of melt pockets

We also considered the possibility that anisotropy in the Ryukyu wedge arises not from lattice preferred orientation due to dislocation creep in olivine, but from shape preferred orientation of melt structures. The contribution of aligned melt to anisotropy in the mantle has been examined by Kendall (1994) for the case of a mid-ocean ridge, by Kendall and Silver (1998) and Moore et al. (2004) for the D'' region, and by Fischer et al. (2000) for a subduction zone. Fischer et al. (2000) considered a model in which melt-filled cracks align $20\text{--}30^\circ$ from the maximum deviatoric compressive stress, following the experimental results of Zimmerman et al. (1999), and concluded that melt-filled cracks could result in trench-parallel splitting. However, melt production in subduction zones is likely restricted to a thin column of vertical melt transport (see, for example, Gaetani and Grove, 2003) and therefore anisotropy due to aligned melt structures would have to be concentrated in a small zone directly beneath the stations to explain both the teleseismic and local splitting for Ryukyu. It is unlikely a very small volume of SPO-induced anisotropy can explain the large split times (up to 2 s, with an average δt of about 1 s) observed in this study. Also, it is unclear what processes control the geometry of melt migration in subduction zones, and where (or whether) aligned melt cracks or sheets are likely to form. We therefore conclude that the melt hypothesis is unlikely for Ryukyu, but further work on the aligned melt hypothesis is needed to rule out this possibility completely.

5.4. Frozen anisotropy in the lithosphere and/or crust

Finally, we examined the hypothesis that the splitting we observe is due to frozen anisotropy in the lithosphere or crust and is unrelated to present-day deformation processes. Some contribution to the observed signal from the crust is likely in this splitting dataset, but anisotropy in the crust cannot explain the observed δt values up

to nearly 2 s. The crustal thickness in the Ryukyu arc, ~35–40 km (Taira, 2001), is insufficient to explain such large splitting, and observed crustal splitting times in Japan average about 0.2 s (Kaneshima, 1990). It has been demonstrated that both lithospheric and asthenospheric contributions to anisotropy are important in many regions (e.g., Fouch et al., 2000; Simons et al., 2002; Simons and van der Hilst, 2003; Fischer et al., 2005; Waite et al., 2005), although splitting measurements in subduction zone settings are nearly always interpreted in terms of flow in the asthenosphere (e.g., Fischer et al., 1998, 2000; Smith et al., 2001; Anderson et al., 2004). The lithosphere beneath the Ryukyu arc stations is likely to be thin, due to thermal erosion associated with mantle wedge flow (e.g., Conder et al., 2002), and it is unlikely that the lithosphere is thick enough to explain the large split times. A second line of argument against primarily lithospheric anisotropy comes from the data itself. As argued in Long and van der Hilst (2005a), for *F*-net stations with simple teleseismic splitting patterns, such as the Ryukyu arc stations, we expect little or no contribution from the lithosphere, or that the fast directions in the lithosphere and the asthenosphere are closely aligned. Therefore, although we cannot completely rule out a contribution from the lithosphere, the anisotropic signal we observe is probably dominated by present-day deformation and flow in the asthenosphere.

5.5. *The most plausible model for Ryukyu anisotropy*

All of the models considered here have some weaknesses when considered in the context of the Ryukyu arc splitting dataset. However, we conclude that the most likely explanation for the trench-parallel anisotropy in the wedge is a model that combines corner flow in the wedge with a B-type olivine fabric. Although we observe trench-parallel fast directions farther into the backarc than predicted by early modeling work on the B-type hypothesis (Kneller et al., 2005), we think it is possible that our splitting results can be reconciled with such models by an adjustment of model parameters or scaling relations of laboratory results. The B-type fabric model may also be consistent with the minority of trench-perpendicular and intermediate fast directions observed in part of the dataset if the associated raypaths sample regions of the backarc mantle that are dominated by A-, C-, or E-type fabric, or if they sample the transition region between the fabric regimes. There is also likely a small amount of splitting signal from anisotropy in the crust, which may explain the increased scatter in the high-frequency splitting dataset.

If the B-type fabric hypothesis is, indeed, the correct explanation for the trench-parallel fast directions we observe in Ryukyu, then our results suggest that the physical range in which B-type fabric can develop may be larger than that suggested by the modeling results of Kneller et al. (2005) and/or the laboratory results of Jung and Karato (2001). New experimental data on olivine fabrics in pressure-temperature-water content space (e.g. Katayama and Karato, 2006), observations of B-type fabric in natural rocks (e.g. Skemer et al., 2006), and models of strain accumulation in the proposed B-type fabric regime should shed further light on the viability of the B-type fabric hypothesis. It has not yet been demonstrated, however, that B-type fabrics can indeed develop over the large region that the Ryukyu splitting observations would require. Additionally, models must demonstrate that sufficient strains can be accumulated in the B-type fabric-dominated regime to produce the relatively large split times that we observe in this study.

6. Summary

We measured shear wave splitting from local events in the Ryukyu arc and compared these measurements to a previously published set of teleseismic splitting observations at the same stations. We obtained 70 high-quality measurements and found that a majority of fast directions lie within 20° of the strike of the trench, although a significant minority exhibit φ values that are trench-perpendicular or intermediate. The local splitting trends are similar to the teleseismic splitting observed by Long and van der Hilst (2005a). From these observations, we infer that there is significant trench-parallel anisotropy in the Ryukyu mantle wedge. After exploring several plausible explanations for this observation, we favor a model in which anisotropy develops due to strain associated with corner flow in the mantle wedge, and B-type olivine lattice preferred orientation dominates.

Acknowledgements

We acknowledge the Japanese National Research Institute for Earth Science and Disaster Prevention as the source for the data used in this study. We thank James Conder, Martijn de Hoop, Brad Hager, Tim Grove, Stephane Rondenay, and Wiki Royden for useful discussions, and Sara Pozgay for her comments on an early draft of this manuscript. We thank Vadim Levin and an anonymous reviewer for their thoughtful and helpful reviews. This work was supported by NSF grant EAR-0337697.

References

- Alsina, D., Snieder, R., 1995. Small-scale sublithospheric continental mantle deformation: constraints from SKS splitting observations. *Geophys. J. Int.* 123, 431–448.
- Anderson, M.L., Zandt, G., Triep, E., Fouch, M., Beck, S., 2004. Anisotropy and mantle flow in the Chile-Argentina subduction zone from shear wave splitting analysis. *Geophys. Res. Lett.* 31, L23608, doi:10.1029/2004GL020906.
- Ando, M., Ishikawa, Y., Yamazaki, F., 1983. Shear wave polarization anisotropy in the upper mantle beneath Honshu, Japan. *J. Geophys. Res.* 88, 5850–5864.
- Buttles, J., Olson, P., 1998. A laboratory model of subduction zone anisotropy. *Earth Planet. Sci. Lett.* 164, 245–262.
- Clitheroe, G., van der Hilst, R.D., 1998. Complex anisotropy in the Australian lithosphere from shear-wave splitting in broad-band SKS records. In: Braun, J., Dooley, J., Goleby, B., van der Hilst, R., Klootwijk, C. (Eds.), *Structure and Evolution of the Australian Continent*, Am. Geophys. Union, Geodyn. Ser., vol. 26.
- Conder, J.A., Wiens, D.A., Morris, J., 2002. On the decompression melting structure at volcanic arcs and back-arc spreading centers. *Geophys. Res. Lett.* 29, doi:10.1029/2002GL015390.
- Currie, C.A., Cassidy, J.F., Hyndman, R.D., Bostock, M.G., 2004. Shear wave anisotropy beneath the Cascadia subduction zone and western North American craton. *Geophys. J. Int.* 157, 341–353.
- Engdahl, E.R., van der Hilst, R.D., Buland, R.P., 1998. Global teleseismic earthquake relocation from improved travel times and procedures for depth determination. *Bull. Seism. Soc. Am.* 88, 722–743.
- Flesch, L.M., Holt, W.E., Silver, P.G., Stephenson, M., Wang, C.-Y., Chan, W.W., 2005. Constraining the extent of crust-mantle coupling in central Asia using GPS, geologic, and shear wave splitting data. *Earth Planet. Sci. Lett.* 238, 248–268.
- Fischer, K.M., Wiens, D.A., 1996. The depth distribution of mantle anisotropy beneath the Tonga subduction zone. *Earth Plane. Sci. Lett.* 164, 245–262.
- Fischer, K.M., Fouch, M.J., Wiens, D.A., Boettcher, M.S., 1998. Anisotropy and flow in Pacific subduction zone back-arcs. *Pure Appl. Geophys.* 151, 463–475.
- Fischer, K.M., McCarthy, C.M., Zaranek, S.E., Rychert, C.A., Li, A., 2005. Asthenospheric anisotropy beneath North America. *Eos Trans. AGU*, 86 (52), Fall Meet. Suppl. (Abstract U52A-01).
- Fischer, K.M., Parmentier, E.M., Stine, A.R., Wolf, E.R., 2000. Modeling anisotropy and plate-driven flow in the Tonga subduction zone back arc. *J. Geophys. Res.* 105, 16,181–16,191.
- Fouch, M.J., Fischer, K.M., 1996. Mantle anisotropy beneath northwest Pacific subduction zones. *J. Geophys. Res.* 101, 15987–16002.
- Fouch, M.J., Fischer, K.M., 1998. Shear wave anisotropy in the Mariana subduction zone. *Geophys. Res. Lett.* 25, 1221–1224.
- Fouch, M.J., Fischer, K.M., Wyssession, M.W., Clark, T.J., 2000. Shear wave splitting, continental keels, and patterns of mantle flow. *J. Geophys. Res.* 105, 6255–6276.
- Fouch, M.J., Silver, P.G., Bell, D.R., Lee, J.N., 2004. Small-scale variations in seismic anisotropy near Kimberley, South Africa. *Geophys. J. Int.* 157, 764–774.
- Fournier, M., Fabbri, O., Angelier, J., Cadet, J.-P., 2001. Regional seismicity and on-land deformation in the Ryukyu arc: Implications for the kinematics of opening of the Okinawa Trough. *J. Geophys. Res.* 106, 13,751–13,768.
- Fukao, Y., 1984. Evidence from core-reflected shear waves for anisotropy in the Earth's mantle. *Nature* 309, 695–698.
- Gaetani, G.A., Grove, T.L., 2003. Experimental constraints on melt generation in the mantle wedge. In: Eiler, J.M. (Ed.), *Inside the Subduction Factory*. Am. Geophys. Union, Geophys. Monogr. Ser., vol. 138.
- Gorbatov, A., Kennett, B.L.N., 2003. Joint bulk-sound and shear tomography for Western Pacific subduction zones. *Earth Planet. Sci. Lett.* 210, 527–543.
- Gripp, A.E., Gordon, R.G., 2002. Young tracks of hot spots and current plate velocities. *Geophys. J. Int.* 150, 321–361.
- Gudmundsson, O., Sambridge, M., 1998. A regionalized upper mantle (RUM) seismic model. *J. Geophys. Res.* 103, 7121–7136.
- Hall, C., Fischer, K.M., Parmentier, E.M., Blackman, D.K., 2000. The influence of plate motions on three-dimensional back arc mantle flow and shear wave splitting. *J. Geophys. Res.* 105, 28,009–28,033.
- Heuret, A., Lallemand, S., 2005. Plate motions, slab dynamics and back-arc deformation. *Phys. Earth Planet. Inter.* 149, 31–51.
- Iwasaki, T., Hirata, N., Kanazawa, T., Melles, J., Suyehiro, K., Urabe, T., Moeller, L., Makris, J., Shimamura, H., 1990. Crustal and upper mantle structure in the Ryukyu Island Arc deduced from deep seismic sounding. *Geophys. J. Int.* 102, 631–657.
- Jung, H., Karato, S.-i., 2001. Water-induced fabric transitions in olivine. *Science* 293, 1460–1463.
- Kaneshima, S., 1990. Origin of crustal anisotropy: shear wave splitting studies in Japan. *J. Geophys. Res.* 95, 11121–11133.
- Kao, H., Huang, G.-C., Liu, C.-S., 2000. Transition from oblique subduction to collision in the northern Luzon arc-Taiwan region: Constraints from bathymetry and seismic observations. *J. Geophys. Res.* 105, 3059–3079.
- Karato, S.-i., 2003. Mapping water content in the upper mantle. In: Eiler, J.M. (Ed.), *Inside the Subduction Factory*. Am. Geophys. Union, Geophys. Monogr. Ser., vol. 138.
- Katayama, I., Karato, S.-i., 2006. Effects of temperature and stress on the deformation fabrics of olivine under hydrous conditions: an experimental study. *Earth Planet. Sci. Lett.*, submitted for publication.
- Kendall, J.-M., 1994. Teleseismic arrivals at a mid-ocean ridge: effects of mantle melt and anisotropy. *Geophys. Res. Lett.* 21, 301–304.
- Kendall, J.-M., Silver, P.G., 1998. Investigating causes of D' anisotropy. In: Gurnis, M., Wyssession, M.E., Knittle, E., Buffett, B.A. (Eds.), *The Core-mantle Boundary Region*, Am. Geophys. Union, Geodyn. Ser., vol. 28.
- Kendall, J.-M., Stuart, G.W., Ebinger, C.J., Bastow, I.D., Keir, D., 2005. Magma-assisted rifting in Ethiopia. *Nature* 433, 146–148.
- Kneller, E.A., van Keken, P.E., Karato, S.-i., Park, J., 2005. B-type olivine fabric in the mantle wedge: Insights from high-resolution non-Newtonian subduction zone models. *Earth Planet. Sci. Lett.* 237, 781–797.
- Kubo, A., Fukuyama, E., 2003. Stress field along the Ryukyu Arc and the Okinawa Trough inferred from moment tensors of shallow earthquakes. *Earth Planet. Sci. Lett.* 210, 305–316.
- Lallemand, S., Liu, C.-S., Dominguez, S., Schnuerle, P., Malavieille, J., 1999. Trench-parallel stretching and folding of forearc basins and lateral migration of the accretionary wedge in the southern Ryukyus: a case of strain partition caused by oblique convergence. *Tectonics* 18, 231–247.
- Lebedev, S., Nolet, G., 2003. Upper mantle beneath Southeast Asia from S velocity tomography. *J. Geophys. Res.* 108, 2048, doi:10.1029/2000JB000073.
- Letouzey, J., Kimura, M., 1985. Okinawa Trough genesis: structure and evolution of a backarc basin developed in a continent. *Marine Petrol. Geol.* 2, 111–130.

- Lev, E., Long, M.D., van der Hilst, R.D., 2006. Seismic anisotropy in eastern Tibet from shear wave splitting: possible evidence for crust-mantle decoupling. *Earth Planet. Sci. Lett.*, submitted for publication.
- Levin, V., Droznin, D., Park, J., Gordeev, E., 2004. Detailed mapping of seismic anisotropy with local shear waves in southeastern Kamchatka. *Geophys. J. Int.* 158, 1009–1023.
- Levin, V., Menke, W., Park, J., 1999. Shear wave splitting in the Appalachians and the Urals: a case for multilayered anisotropy. *J. Geophys. Res.* 104, 17975–17993.
- Li, C., van der Hilst, R.D., Toksöz, M.N., 2006. Constraining P-wave velocity variations in the upper mantle beneath Southeast Asia. *Phys. Earth Planet. Inter.* 154, 180–195.
- Long, M.D., van der Hilst, R.D., 2005a. Upper mantle anisotropy beneath Japan from shear wave splitting. *Phys. Earth Planet. Inter.* 151, 206–222.
- Long, M.D., van der Hilst, R.D., 2005b. Estimating shear-wave splitting parameters from broadband recordings in Japan: a comparison of three methods. *Bull. Seism. Soc. Am.* 95, 1346–1358.
- Marson-Pidgeon, K., Savage, M.K., 1997. Frequency-dependent anisotropy in Wellington, New Zealand. *Geophys. Res. Lett.* 24, 3297–3300.
- Marson-Pidgeon, K., Savage, M.K., Gledhill, K., Stuart, G., 1999. Seismic anisotropy beneath the lower half of the North Island, New Zealand. *J. Geophys. Res.* 104, 20277–20286.
- Mazzotti, S., 1999. L'arc insulaire japonais: déformation transitoire et permanente liée à la subduction et à la collision. PhD Thesis, Université Paris-Sud, Orsay-Paris XI.
- McCaffrey, R., 1996. Estimates of modern arc-parallel strain rates in forearcs. *Geology* 24, 27–30.
- Mehl, L., Hacker, B.R., Hirth, G., Kelemen, P.G., 2003. Arc-parallel flow within the mantle wedge: evidence from the accreted Talkeetna arc, south central Alaska. *J. Geophys. Res.* 108, 2375, doi:10.1029/2002JB002233.
- Mizukami, T., Wallis, S.R., Yamamoto, J., 2004. Natural examples of olivine lattice preferred orientation patterns with a flow-normal a -axis maximum. *Nature* 427, 432–436.
- Moore, M.M., Garnero, E.J., Lay, T., Williams, Q., 2004. Shear wave splitting and waveform complexity for lowermost mantle structures with low-velocity lamellae and transverse isotropy. *J. Geophys. Res.* 109, doi:10.1029/2003JB002546.
- Nakajima, J., Hasegawa, A., 2004. Shear-wave polarization anisotropy and subduction-induced flow in the mantle wedge of northern Japan. *Earth Planet. Sci. Lett.* 225, 365–377.
- Özalaybey, S., Chen, W.-P., 1999. Frequency-dependent analysis of SKS/SKKS waveforms observed in Australia: evidence for null birefringence. *Phys. Earth Planet. Inter.* 114, 197–210.
- Özalaybey, S., Savage, M.K., 1995. Shear-wave splitting beneath western United States in relation to plate tectonics. *J. Geophys. Res.* 100, 18135–18149.
- Park, J., Levin, V., 2002. Seismic anisotropy: tracing plate dynamics in the mantle. *Science* 296, 485–489.
- Peyton, V., Levin, V., Park, J., Brandon, M., Lees, J., Gordeev, E., Ozerov, A., 2001. Mantle flow at a slab edge; seismic anisotropy in the Kamchatka region. *Geophys. Res. Lett.* 28, 379–382.
- Russo, R.M., Silver, P.G., 1994. Trench-parallel flow beneath the Nazca Plate from seismic anisotropy. *Science* 263, 1105–1111.
- Ryberg, T., Rumpker, G., Haberland, C., Stromeyer, D., Weber, M., 2005. Simultaneous inversion of shear wave splitting observations from seismic arrays. *J. Geophys. Res.* 110, doi:10.1029/2004JB003303.
- Saltzer, R.L., Gaherty, J., Jordan, T.H., 2000. How are vertical shear wave splitting measurements affected by variations in the orientation of azimuthal anisotropy with depth? *Geophys. J. Int.* 141, 374–390.
- Sandvol, E., Ni, J., 1997. Deep azimuthal seismic anisotropy in the southern Kurile and Japan subduction zones. *J. Geophys. Res.* 102, 9911–9922.
- Schellart, W.P., Lister, G.S., Jessell, M.W., 2002. Analogue modelling of asymmetrical back-arc extension. *J. Virtual Explorer* 7, 25–42.
- Simons, F.J., van der Hilst, R.D., Montagner, J.-P., Zielhuis, A., 2002. Multimode Rayleigh wave inversion for heterogeneity and azimuthal anisotropy of the Australian upper mantle. *Geophys. J. Int.* 151, 738–755.
- Simons, F.J., van der Hilst, R.D., 2003. Anisotropic structure and deformation of the Australian lithosphere. *Earth Planet. Sci. Lett.* 211, 271–286.
- Skemer, P., Katayama, I., Karato, S.-i., 2006. Peridotite deformation fabrics from Cima di Gagnone, Central Alps, Switzerland: evidence of deformation under water-rich conditions at low temperatures. *Contrib. Mineral. Petr.*, submitted for publication.
- Smith, W.H.F., Sandwell, D.T., 1997. Global seafloor topography from satellite altimetry and ship depth soundings. *Science* 277, 1957–1962.
- Smith, G.P., Wiens, D.A., Fischer, K.M., Dorman, L.M., Webb, S.C., Hildebrand, J.A., 2001. A complex pattern of mantle flow in the Lau Backarc. *Science* 292, 713–716.
- Taira, A., 2001. Tectonic evolution of the Japanese Island arc system. *Annu. Rev. Earth Planet. Sci.* 29, 109–134.
- Walker, K.T., Bokelmann, G.H.R., Klemperer, S.L., 2001. Shear-wave splitting to test mantle deformation models around Hawaii. *Geophys. Res. Lett.* 28, 4319–4322.
- Waite, G.P., Schutt, D.L., Smith, R.B., 2005. Models of lithosphere and asthenosphere anisotropic structure of the Yellowstone hot spot from shear wave splitting. *J. Geophys. Res.* 110, B11304, doi:10.1029/2004JB003501.
- Wang, T.K., Lin, S.-F., Liu, C.-S., Wang, C.-S., 2004. Crustal structure of the southernmost Ryukyu subduction zone: OBS, MCS and gravity modelling. *Geophys. J. Int.* 157, 147–163.
- Widiyantoro, S., Kennett, B.L.N., van der Hilst, R.D., 1999. Seismic tomography with P and S data reveals lateral variations in the rigidity of deep slabs. *Earth Planet. Sci. Lett.* 173, 91–100.
- Wiens, D.A., Smith, G.P., 2003. Seismological constraints on structure and flow patterns within the mantle wedge. In: Eiler, J.M. (Ed.), *Inside the Subduction Factory*. Am. Geophys. Union, Geophys. Monogr. Ser., vol. 138.
- Wolfe, C.J., Solomon, S.C., 1998. Shear-wave splitting and implications for mantle flow beneath the MELT region of the East Pacific Rise. *Science* 280, 1230–1232.
- Xue, M., Allen, R.M., 2005. Asthenospheric channeling of the Icelandic upwelling: evidence from seismic anisotropy. *Earth Planet. Sci. Lett.* 235, 167–182.
- Yang, X., Fischer, K.M., Abers, G., 1995. Seismic anisotropy beneath the Shumagin Islands segment of the Aleutian-Alaska subduction zone. *J. Geophys. Res.* 100, 18165–18177.
- Yu, S.B., Kuo, L.C., 1996. GPS observations of crustal deformation in the Taiwan-Luzon region. *Geophys. Res. Lett.* 26, 923–926.
- Zimmerman, M.E., Zhang, S., Kohlstedt, D.L., Karato, S.-i., 1999. Melt distribution in mantle rocks deformed in shear. *Geophys. Res. Lett.* 26, 1505–1508.